Journal of Colloid and Interface Science 343 (2010) 564–573

Contents lists available at ScienceDirect

Journal of Colloid and Interface Science

www.elsevier.com/locate/jcis

Electric permittivity of concentrated suspensions of elongated goethite particles

R.A. Rica, M.L. Jiménez, A.V. Delgado *

Department of Applied Physics, School of Sciences, Campus Fuentenueva, University of Granada, 18071 Granada, Spain

ARTICLE INFO

Article history:
Received 3 November 2009
Accepted 27 November 2009
Available online 4 December 2009

Keywords:
Alpha relaxation
Concentrated suspensions
Electric permittivity
Electrokinetics
Goethite
Spheroidal particles

ABSTRACT

This paper describes an investigation on the electric permittivity of concentrated suspensions of nonspherical particles, specifically prolate spheroids. It is first discussed how the determination of the frequency (ω) dependence of the electric permittivity (a phenomenon traditionally known as LFDD or low-frequency dielectric dispersion) can provide ample information on the properties of the dispersed material (shape, size, state of aggregation, conductivity) and of its interface with the (typically aqueous) medium. The basic quantities are the strength and frequency dependence of the dipole moment induced by the applied field, and its dimensionless counterpart, the dipole coefficient, $C^*(\omega)$. It is explicitly shown how the (complex) relative permittivity of the suspension, $\varepsilon_r^*(\omega)$, can be calculated from it. Two theoretical models on the polarizability of spheroidal colloidal particles will be used as theoretical starting point; one of them (Model I) explicitly considers two relaxations of the permittivity, each associated to one of the particle axes. The other (Model II) is a semi-analytical theory that yields an LFDD practically independent of the axial ratio of the particles. Both models are aimed to be used if the suspensions are dilute (low volume fraction of solids, ϕ), and here they are generalized to concentrated systems by means of a previously published approximate evaluation of the permittivity of concentrated suspensions. Experiments are performed in the 1 kHz–1 MHz frequency range on suspensions of elongated goethite particles; the effects of ionic strength, pH, and volume fraction are investigated, and the two models are fitted to the data. In reality, taking into account that the particles are non-uniformly charged (a fact that contributes to their instability), two zeta potentials (roughly representing the lateral surface and the tip of the spheroid) are used as parameters. The results indicate that, when experimental conditions are optimal (high ionic strength and low zeta potential), the suspensions do indeed display two relaxations, that we ascribe to the long axis (and to flocs likely present in suspension) and to the short one. The permittivity increases with ionic strength, a result found with other systems, and compatible with a zeta potential that, on the average, decreases with ionic strength, an equally well known result, consequence of electric double layer compression. Another reasonable finding is the increase of estimated average dimensions and the decrease of electrokinetic potentials when the pH is close to the isoelectric point of goethite (around pH 9). The increase in volume fraction, finally, produces an overall increase in the permittivity, and the approximate model used for the evaluation of volume fraction variations can describe properly these effects, with basically constant zeta potentials and dimensions.

1. Introduction

The electrokinetics of concentrated colloidal suspensions of nonspherical particles has received limited attention, considering the experimental and theoretical difficulties involved. Shape effects are very often neglected in the investigation of disperse systems, as nonspherical "model" particles (with controlled geometry, polydispersity and composition) are not readily accessible, unlike spheres, many of them commercially available. In addition, the theoretical description of electrokinetic phenomena in suspensions of particles with geometry other than spherical (spheroidal, cylindrical, planar) although developed under certain limiting situations in the past [1,2], has quite recently received attention and an exact description [3,4]. For that reason, the scarce existing experimental data have typically been described in terms of qualitative models or under the assumption that an equivalent-sphere formulation suffices, something strictly valid only in the so-called Smoluchowski limit (low surface conductivity, and electric double layer thickness much smaller than the particle radius).

The information is even more limited if we consider the more technologically interesting case of concentrated suspensions. In this case, there are only some experimental investigations on clays [5], which take advantage of electro-acoustic techniques [6] allowing the determination of the electrophoretic mobility of

* Corresponding author. Departamento de Física Aplicada, Facultad de Ciencias, Campus Fuentenueva, Universidad de Granada, Departamento de Física Aplicada, Universidad de Granada, 18071 Granada, Spain. Fax: +34 958 24 32 14.
E-mail addresses: rul@ugr.es (R.A. Rica), jimenezo@ugr.es (M.L. Jiménez), adelgado@ugr.es (A.V. Delgado).

0021-9797/$ - see front matter © 2009 Elsevier Inc. All rights reserved.
doi:10.1016/j.jcis.2009.11.063

concentrated suspensions in alternating electric fields (the dynamic mobility). Available instruments and theoretical models have the capability of calculating both the zeta potential and average size (assuming spherical shape) of the particles in concentrated slurries, as usually found in natural soils or technological applications. However, the assumption of sphericity has been shown to lead to erroneous particle sizes [6] and a consequently poor characterization of the particles is obtained. Notwithstanding these limitations, correct characterizations are mandatory for many applications [7], in which an exact knowledge of the electrical state of the particle surface, and from this the electrostatic interaction between particles, is a necessary requirement.

Here it should be mentioned that there is another electrokinetic phenomenon which is related to electro-acoustics in the sense that it is based on the application of alternating fields, and that measures a collective property of the suspension. This is the so called low-frequency dielectric dispersion (LFDD), which consists of the evaluation of the electric permittivity of a colloidal suspension as a function of the frequency of the electric field. This phenomenon has been shown to be very sensitive to the polarization state of the solid–liquid interface and the properties of the particles themselves [1,8–12]. Again in this case, neither theoretical nor experimental works exist dealing with concentrated suspensions of nonspherical particles, and only some studies concerning dilute systems (spheroidal [13] or planar [14,15] particles) have been reported.

One of the mathematical complications involved in the theoretical evaluation of electrokinetics in such geometries is the description of the polarization of the electrical double layer (EDL) of the particles in the presence of an alternating electric field. The full solution of this problem was recently made available numerically by Fixman [3] in the case of dilute suspensions, and analytical or semi-analytical treatments are also available in some situations [16,17]. Any correct analysis should predict at least two main relaxation processes in the frequency dependence of the EDL polarization (and hence of the electric permittivity). On one hand, the δ or Maxwell–Wagner-O'Konski (MWO) relaxation process appears typically in the MHz frequency range, and it is hence especially important in electro-acoustic experiments, as they are mostly suited to be used in that range. The MWO process is due to the mismatch of both permittivity and conductivity values between particles and solution [10], and it is usually of minor importance in dielectric measurements, considering that the amplitude of the associated relaxation tends to be low.

In fact, the main contribution to the dielectric relaxation processes in suspensions comes from another mechanism: it is related to the concentration polarization phenomenon. We are referring to the field-induced concentration gradient of neutral electrolyte on both sides of the particle along the direction of the field. We will give a very short description here (see Refs. [1,2,10,11] for more details). Consider a particle bearing a negative surface charge, dispersed in an electrolyte solution. Assume that an electric field (stationary, at the moment) is applied in the $+z$ direction (from left to right of the page, say), inducing fluxes of ions both in the bulk solution and in the EDL. Because the double layer is enriched in counterions (cations in the case considered), the field will drive them towards the right hand side of the particle; in solution, the concentration of counterions is smaller than it is in the EDL, so the counterions brought tangentially by the field in the EDL cannot be driven at the same rate in the bulk. Conversely, coions are driven from the bulk to the right hand side of the particle; because they are so scarce in the EDL, their flux will be considerably reduced there. As a consequence, both counterions (cations) and coions (anions) are accumulated on that side: briefly, one can say that excess EDL cations cannot travel into the bulk, and coions from the bulk cannot go into the EDL. We are faced with an increase in neutral salt concentration on the right and a subsequent decrease on the opposite side (the concentration polarization). The characteristic dimension of the region at which such accumulation and depletion occur is comparable to the particle size. This polarization induces large diffusion electric currents around the particles, lagging behind the electric field, and these displacement currents are macroscopically observed as an increased electric permittivity.

The characteristic relaxation frequency will be of the order of $2D/\ell^2$, where D is some average diffusion coefficient of ions and ℓ is the characteristic dimension of the concentration perturbation (of the order of the particle size). Assuming a solution of simple ions with a diffusion coefficient of, say, 10^{-9} m^2/s, and a particle dimension $\ell = 150$ nm, the α-relaxation will occur at about 9×10^4 rad/s or 14 kHz. This is the reason why this process is considered a low-frequency one (as compared to the MWO relaxation -or to molecular or atomic relaxations, occurring at still higher frequencies), and hence the denomination of low-frequency dielectric dispersion (LFDD) given to the frequency dependence of the permittivity in this region. Note that when the field frequency is sufficiently above that value, the concentration gradient cannot be built, and the electric permittivity relaxes to its high frequency value [9,10]. When the particles have two or more characteristic size parameters, like the two axial dimensions in spheroids, the problem involves the additional difficulty of distinguishing the contributions of ionic fluxes in either axis direction, and how these fluxes contribute to the observed experimental behavior.

It is worth to mention that, important as this relaxation is for the permittivity of the suspension, it bears little significance in dynamic mobility determinations, where the MWO and the inertia processes are dominant. It can thus be said that LFDD and electro-acoustic techniques are appropriate to be used in different frequency ranges and can be considered as complementary electrokinetic tools [18].

All the above mentioned models assume that the suspensions are dilute. It is of interest to extend their calculations to account for particle–particle interactions and thus make them applicable to concentrated dispersions. Since a general model of the electrokinetics in suspensions of concentrated non-spherical particles is lacking, we propose in this paper the use of an approximate semi-analytical model, reported by Delgado et al. [19]. These authors described the corrections that were required in electric permittivity calculations in order to take into account that the suspensions are moderately concentrated in solids. Although specifically elaborated for spheres, the model is based on such general arguments that it may be adequate to apply them to spheroids, at least for not too large axial ratios. In a recent work [20] we suggested a similar approach for the analysis of the electro-acoustic response of concentrated suspensions of prolate spheroids, both experimentally and theoretically.

Our aim in this paper is to contribute to our knowledge of the LFDD of spheroidal particles, applying the technique to suspensions of elongated goethite (β-FeOOH) moderately concentrated in solids. Electric permittivity determinations will be presented, considering the effects of the volume fraction of solids, the pH, and the ionic strength of the medium. These experimental data will be compared to the predictions of existing models for the low-frequency polarization effects in dilute suspensions of spheroids [16,17], that will be extended so as to include interactions among particles by means of the semi-analytical formula reported in Ref. [19].

2. Theoretical background

In this work, two approximations to the electric permittivity of concentrated suspensions of prolate colloidal spheroids are made.

It will be clear from our previous comments that the fundamental physical quantity required for the description of the electric permittivity of disperse systems is the strength $\mathbf{d}\exp(-j\omega t)$ $(j=\sqrt{-1})$ of the dipole induced in the particles (including their EDLs) by the applied alternating field of frequency ω, $\mathbf{E}_0\exp(-j\omega t)$. This dipole will be characterized by its dimensionless dipole coefficient C^*, carrying information about the polarizability of the particle. The relationship between $\mathbf{d}$ and C^* is, for the case of a prolate spheroid with semiaxes a and b (a is the long semiaxis, or half the dimension of the particle along its symmetry axis; b is the short semiaxis, or half the dimension perpendicularly to the symmetry axis):

$$\mathbf{d}^i = 4\pi\varepsilon_0\varepsilon_{rm}ab^2C^{*,i}\mathbf{E}_0 = 4\pi\varepsilon_0\varepsilon_{rm}ab^2(C_1^i - jC_2^i)\mathbf{E}_0 \tag{1}$$

where $i=\parallel,\perp$ corresponds, respectively, to parallel and perpendicular orientation of the long axis with respect to the field. Here ε_0 is the permittivity of vacuum, and ε_{rm} is the relative permittivity of the medium. In this equation, the complex character of the dipole coefficient has been explicitly taken into account (for convenience, its real and imaginary components will be denoted C_1^i and $-C_2^i$, respectively). As will be shown below, it is the frequency dispersion of this coefficient that determines the LFDD of the suspension, and, to a large extent, also the frequency dependence of the dynamic mobility. In addition, its zero frequency value is also determinant of the electrophoretic mobility of the particles. From this it will be clear how important it is the evaluation of the dipole coefficient in any rigorous description of electrokinetics [21–23].

We will make use of two previous models of the induced dipole coefficient of spheroids in dilute suspensions, and extend them in order to make the models applicable to systems with high concentrations of solids. From the first model, based on a work by Grosse et al. [16] (Model I hereafter), expressions for the dielectric increment at zero frequency (see below), characteristic time of the α-relaxation and limiting (static and high-frequency) values of the dipole coefficient can be obtained for arbitrary values of the zeta potential and the axial ratio r ($r=b/a$), in the traditionally called thin double layer approximation. This means that the thickness of the double layer, κ^{-1}, is much smaller than the smallest dimension of the particle (b in the case of prolate spheroids):

$$\kappa b \gg 1$$
$$\kappa = \left(\frac{\sum_{\alpha=1}^{N} 10^3 N_A c_\alpha e^2 z_\alpha^2}{\varepsilon_{rm}\varepsilon_0 k_B T}\right)^{1/2} \tag{2}$$

where κ, the Debye-Hückel parameter (reciprocal Debye length), depends on the molar concentrations c_α, and the valencies z_α of the N ionic species in solution. In Eq. (2), N_A is the Avogadro number, e is the elementary charge, k_B is Boltzmann's constant and T is the absolute temperature.

The second model is based on a recent work by Chassagne and Bedeaux [17] (Model II in what follows), where the authors provide a formula for the dipole coefficient of a spheroidal particle for monovalent, symmetric electrolyte, both ions having identical diffusion coefficients $D^+ = D^- \equiv D$. The only restriction of this model is $\kappa b \geqslant 1$, a condition very often fulfilled in practice.

The quantity of interest, considering experimental evaluation, is the dielectric increment, $\delta\varepsilon_r^*(\omega)$, a complex quantity which measures to what extent the relative permittivity of the suspension, $\varepsilon_r^*(\omega)$, differs from its high-frequency value:

$$\delta\varepsilon_r^*(\omega) = \varepsilon_r^*(\omega) - \varepsilon_r^*(\infty) \tag{3}$$

As above mentioned, both models considered in this work assume that the suspensions are dilute (a subscript "d" will be used to take this into account explicitly): Model I provides expressions for the static ($\omega\to 0$) dielectric increment ($\delta\varepsilon_{r,d}(0)$; this is a real quantity) and the characteristic relaxation frequency of the α-dispersion ($\omega_{\alpha,d}$). In addition, the authors consider Debye-like relaxations. Model II, in turn, yields the frequency spectrum of the dipole coefficient. Note that in both cases, orientation effects must be taken into account, as the polarization of the spheroids will be different for parallel and perpendicular orientation. This means that, according to Model I, the dielectric spectrum of the suspension will be given by the following expression:

$$\varepsilon_{r,d}^{*,i}(\omega) = \varepsilon_{rm} + \phi\frac{\Delta\varepsilon_{r,d}^i(0)}{1 + j\omega/\omega_{\alpha,d}^i} \tag{4}$$

where $\Delta\varepsilon_{r,d}^i(0)$ is the dielectric increment per unit volume fraction, and the linear dependence of the dielectric increment on the volume fraction is the manifestation of the fact that this theory is valid for dilute suspensions. The meaning of the superscript "i" was mentioned above (Eq. (1)). In the case of Model II, since only the dipole coefficient is provided (for the two orientations, $C^{*,i}(\omega)$), it is required to establish the relationship between the permittivity and the coefficient. This can be done using the Maxwell model, and the result is [10]:

$$\varepsilon_{r,d}^{*,i}(\omega) = \varepsilon_{rm}\left[1 + 3\phi C^{*,i}(\omega)\right] - j\frac{3\phi K_m}{\omega\varepsilon_0}\left[C^{*,i}(\omega) - C^{*,i}(0)\right] \tag{5}$$

where K_m is the dc conductivity of the medium.

Whatever the model used, it must be added that typically the measurements are performed on suspensions containing randomly oriented spheroids. The calculations for each individual orientation can be easily combined for the random distribution as follows:

$$\delta\varepsilon_{r,d}^*(\omega) = \frac{\delta\varepsilon_{r,d}^{*,\parallel}(\omega) + 2\delta\varepsilon_{r,d}^{*,\perp}(\omega)}{3} \tag{6}$$

This expression can be applied provided the Brownian motion inhibits the tendency of the particles to align in the field direction, a requirement that is achieved if the field strength obeys the following inequality [24,25]:

$$E_0^2 \ll \frac{k_B T}{\varepsilon_{rm}\varepsilon_0 V_p} \tag{7}$$

where V_p is the particle volume. For a rod of length 600 nm and maximum cross sectional diameter 120 nm (the approximate dimensions of our particles) in water and room temperature, this condition requires $E_0 \ll 45\ \mathrm{kV\,m^{-1}}$. In our conductivity cell, the maximum applied field was smaller than $2.5\ \mathrm{Vm^{-1}}$, so this condition is completely fulfilled.

As mentioned above, in order to extend these models to concentrated suspensions, that is, to account for particle–particle interactions, at least approximately, we use a result obtained by Delgado et al. [19], which predicts the following volume fraction dependence of the α-relaxation parameters:

$$\begin{aligned}\delta\varepsilon_r^i(0) &= \delta\varepsilon_{r,d}^i(0)\left(1 + \tfrac{1}{(\phi^{-1/3}-1)^2}\right)^{-3/2}\\ \omega_\alpha^i &= \omega_{\alpha,d}^i\left(1 + \tfrac{1}{(\phi^{-1/3}-1)^2}\right)\end{aligned} \tag{8}$$

It is important to note that these expressions were obtained for monodisperse, uniformly charged spherical particles. Although their application to our elongated, non-uniformly charged rodlike particles is not strictly valid, it allows us to check how important those deviations from a strictly dilute character are for the electrokinetic behavior. Combining the information described on the behavior of dilute systems and the effect of volume fraction, the Model I expression for the frequency spectrum of the dielectric increment of a concentrated suspension of spheroids reads, for random orientation:

$$\delta\varepsilon_r^*(\omega)=\frac{1}{3}\phi\left(1+\frac{1}{(\phi^{-1/3}-1)^2}\right)^{-3/2}\left\{\frac{\delta\varepsilon_{r,d}^{\parallel}(0)}{1+j\omega/\omega_\alpha^{\parallel}}+2\frac{\delta\varepsilon_{r,d}^{\perp}(0)}{1+j\omega/\omega_\alpha^{\perp}}\right\}\text{(Model I)} \tag{9}$$

As mentioned, in the case of Model II, no expressions are available for the frequency dispersion, so the corresponding version of Eq. (9) for that model is:

$$\delta\varepsilon_r^*(\omega)=\frac{1}{3}\phi\left(1+\frac{1}{(\phi^{-1/3}-1)^2}\right)^{-3/2}\left\{\delta\varepsilon_r^{*,\parallel}(\omega)+2\delta\varepsilon_r^{*,\perp}(\omega)\right\}\text{(Model II)} \tag{10}$$

Details on the evaluation of the dielectric increment calculated according to Model I (Model II) are given in Appendix A (Appendix B). Because the experimental spectra are not exactly Debye-like, as has been found many times in different investigations of the LFDD of colloidal systems [26], Eq. (9) was modified, and an empirical Cole–Cole relaxation function was used, as the additional γ parameter permits a better description of the typically wider relaxations shown by actual systems, as compared to the simple Debye one:

$$\delta\varepsilon_r^*(\omega)=\frac{1}{3}\phi\left(1+\frac{1}{(\phi^{-1/3}-1)^2}\right)^{-3/2}\times\left\{\frac{\delta\varepsilon_{r,d}^{\parallel}(0)}{1+(j\omega/\omega_\alpha^{\parallel})^{1-\gamma}}+2\frac{\delta\varepsilon_{r,d}^{\perp}(0)}{1+(j\omega/\omega_\alpha^{\perp})^{1-\gamma}}\right\}\text{(Model I)} \tag{11}$$

3. Experimental

3.1. Materials

Rod-like goethite particles were purchased from Lanxess, USA, under the trade name of Bayferrox-920. As shown in Fig. 1, they have uniform shape and moderate polydispersity. Fitting log-normal distributions to size measurements performed on scanning electron microscope pictures like those in Fig. 1, we obtained $a = (290 \pm 30)$ nm and $b = (50 \pm 6)$ nm for the semiaxes dimensions, giving an axial ratio $r = a/b = 5.8 \pm 0.6$. Light scattering techniques were also used for obtaining the sizes in situ, using the methods and devices described in Ref. [27]. Dynamic light scattering measurements yielded an average hydrodynamic radius of 190 nm, and a value of 175 nm was obtained as radius of gyration using static light scattering [20].

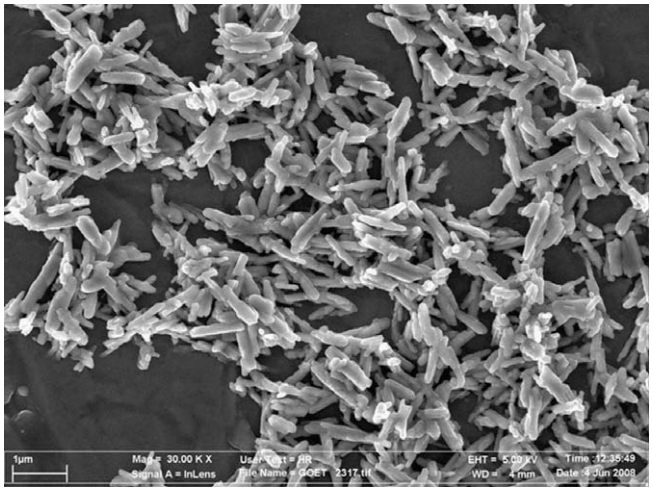

Fig. 1. SEM picture of the goethite particles used. Bar length: 1 μm.

3.2. Methods

The goethite powder was first dispersed in deionized and filtered water (Milli-Q Academic, Millipore, France) at a concentration of about 20 g/L. The suspensions were cleaned by successive cycles of centrifugation and redispersion in water. After this cleaning procedure, aqueous suspensions of goethite particles were prepared with different concentrations of electrolyte (KCl), particle concentrations, and pH values. The suspensions were left to equilibrate for at least 48 h under mechanical stirring. Nevertheless, goethite suspensions with even moderate volume fractions were extremely viscous, as reported by Blakey and James [28], who explained such behavior by considering that goethite particles tend to flocculate in a manner similar to clay particles in water, because the former also have two types of charged groups on their surface. Such groups are not uniformly distributed, and when goethite particles are dispersed at pH 6, their behavior can be explained by assuming that they have both positive and negative charged groups on the lateral surface, and only positive groups and the tips. Like in the case of clay platelets, this non-uniformity will have important consequences on the electrokinetics of this kind of particles. In particular, the high viscosity of goethite suspensions made it difficult working with elevated volume fractions or low particle charge conditions, thus limiting the range of measurements performed to volume fractions up to 8% and pH up to 8.

The permittivity spectra of the suspensions were obtained by measuring the frequency dependence of the impedance of a conductivity cell with parallel, platinized-platinum electrodes at 25.0 ± 0.5 °C, using an HP 4284A (USA) impedance meter, as described in [29]. The main obstacle when performing electric permittivity determinations comes from the electrode–suspension interface. Accumulation of ions occurs in such interface (the so-called electrode polarization, EP), which results in a huge low-frequency contribution to the apparent permittivity of the system. Although different methods are available [8,29–31], measurements were corrected from electrode polarization effects by means of the logarithmic derivative technique [32]. With this method, the contributions to the permittivity of the polarization of both the electrode–solution interface and the suspension are easier to discriminate than in the real or imaginary parts. The logarithmic derivative ε''_{rD} is a quantity whose behavior is very similar to the imaginary part of the electric permittivity, and from which the real part can be easily obtained by integration. Its definition is:

$$\varepsilon''_{rD}(\omega)=\frac{-\pi}{2}\frac{\partial\varepsilon'_r(\omega)}{\partial\ln\omega} \tag{12}$$

Once the data were properly corrected, fits to our two models were made by a least-squares method, which provided the parameters for the electrokinetic characterization of the goethite particles. The steps followed were:

1. Get the impedance vs. frequency data, $Z^*(\omega)$, for a range of distances between the electrodes, in the 5–15 mm interval.
2. From these data, and the cell constant λ previously obtained by using a KCl solution of known electrical conductivity, we can obtain the spectrum of the complex conductivity of the suspension:

$$K^*(\omega)=\frac{\lambda}{Z^*(\omega)} \tag{13}$$

3. From the complex conductivity, the real part of the relative permittivity is obtained as follows [10]:

$$\varepsilon'_r(\omega)=\frac{\mathrm{Im}\{K^*(\omega)\}}{\omega\varepsilon_0} \tag{14}$$

4. Using the definition (12), the logarithmic derivative spectrum is obtained.
5. The data are corrected for electrode polarization as described below. The spectrum of the logarithmic derivative finally ascribed to any system will be the average of the corrected spectra corresponding to the different electrode separations.

4. Results and discussion

4.1. Model predictions

Fig. 2 shows the main features of the behavior of the permittivity of suspensions of randomly oriented spheroids, according to the predictions of the two models. Note, first of all, that both predict evident alpha relaxations, although with significant differences. The low-frequency values of the dielectric increment differ substantially, as a consequence of the different descriptions of the EDL relaxations predicted by each of the two approaches.

According to Model II, a single, wide relaxation with characteristic frequency around 60 kHz is found. The spectra are furthermore practically independent of the axial ratio, r. This is a manifestation of a fundamental hypothesis of the model, according to which the contributions of ionic trajectories in planes perpendicular to the symmetry axis of the prolate spheroid are dominant over those of ions migrating tangentially in the direction parallel to that axis. This means that the only observable relaxation must be that controlled by the size of the small axis, b, which is kept constant in Fig. 2.

On the contrary, Model I considers explicitly two relaxations, each related to one axis length, and in fact two processes (two absorption peaks in Fig. 2b) can be detected if r is sufficiently larger than unity. Additionally, the amplitude of the relaxation increases with r: this is a consequence of the overall increase in particle dimensions: larger dimensions mean larger effects of concentration polarization [33]. Furthermore, the characteristic frequency of the alpha relaxation associated to the long axis shifts to lower values, as expected from the dependence of ω_α on the reciprocal particle size.

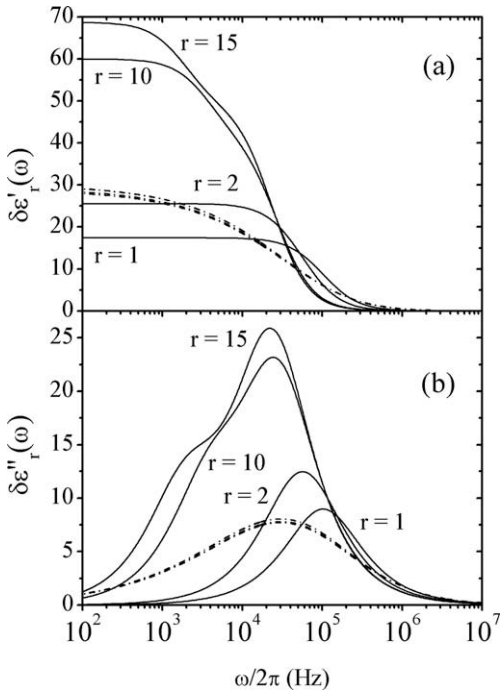

Fig. 2. Real (a) and imaginary (b) parts of the electric permittivity increment of goethite suspensions as a function of the frequency of the applied electric field for different values of the axial ratio $r = a/b$, as predicted by Model I (solid lines) and Model II (dash-dotted lines). Other parameters: 1% volume fraction of solids; zeta potential $\zeta = 100$ mV; $b = 100$ nm; 1 mM KCl.

The models differ even in the $r = 1$ case, but it must be pointed out that Model I assumes thin double layer, while Model II is applicable for virtually any double layer thickness. To this we must add the consideration that the former assumes a Debye relaxation function, and this is not the one that best describes the true relaxation, as mentioned above. The Debye function always yields a steeper permittivity decrease than that found experimentally or in numerical calculations.

The effects of the zeta potential and ionic strength are depicted in Fig. 3. Firstly, we note that $\delta\varepsilon'_r(0)$ increases when either of the two parameters is raised, whereas no change is observed in the characteristic frequency. Regarding the relative importance of the two peaks predicted by Model I, it can be seen that the one associated to the short semiaxis is more important for high ionic strengths and relatively low zeta potentials. This is in agreement with the calculations of Bellini and Mantegazza [34], who showed that, for high frequencies, the differences between the polarizabilities corresponding to parallel and perpendicular orientations increase when the zeta potential increases, with the parallel component always dominating. Thus, at low zeta potential the two contributions are comparable, yielding a wide, single relaxation. When ζ is increased, the surface conductivity raises and so do both polarizabilities, but the parallel orientation produces a faster increase than the perpendicular one. Similarly, when the ionic strength is higher, the differences between both components tend to disappear, and the behavior approaches that of a sphere with a size close to the short semiaxis. It can be said that shape effects are less significant the lower the zeta potential and the higher the ionic strength. This result was partially explored experimentally by Jiménez et al. [35], who showed that two relaxations can be observed in the low-frequency dielectric spectrum of monodisperse elongated hematite particles when the pH of the system is close to the isoelectric point of the particles.

Finally, the effects of the inclusion of a non-zero volume fraction are described in Fig. 4. The effect of ϕ can be summarized by saying that $\delta\varepsilon'_r(0)$ increases with ϕ until reaching a maximum after which it decreases, while ω_α shows a continuous increasing trend. Physically, the maximum expected in $\delta\varepsilon'_r(0)$ is explained by a competition between the enhancement of permittivity due to the larger number of electric double layers and the decrease coming from the overlap between neighbor EDLs. On the other hand, the explanation for the monotonically increasing trend of the characteristic frequency is straightforward if we consider the decreasing volume available to each particle and the subsequent decrease of the diffusion length, which is not the size dimension any more, because the ions encounter the double layer of neighbor particles for distances shorter than ℓ.

4.2. Overall behavior of the electric permittivity of goethite

Examples of raw logarithmic derivative spectra together with data corrected for electrode polarization are shown in Fig. 5. The correction was carried out by subtracting from the raw data an $A\omega^{-3/2}$ contribution associated to the effect of the electrode polarization on the measured permittivity [32]. The constant A was determined by least-squares fitting of the first few low-frequency data points to the $A\omega^{-3/2}$ function. Although part of the true low-frequency dielectric dispersion is thus lost, the information remaining is still sufficient as to characterize the LFDD of the spheroids.

The Figure also includes theoretical predictions according to Models I and II. The best-fitting curves of the two models were

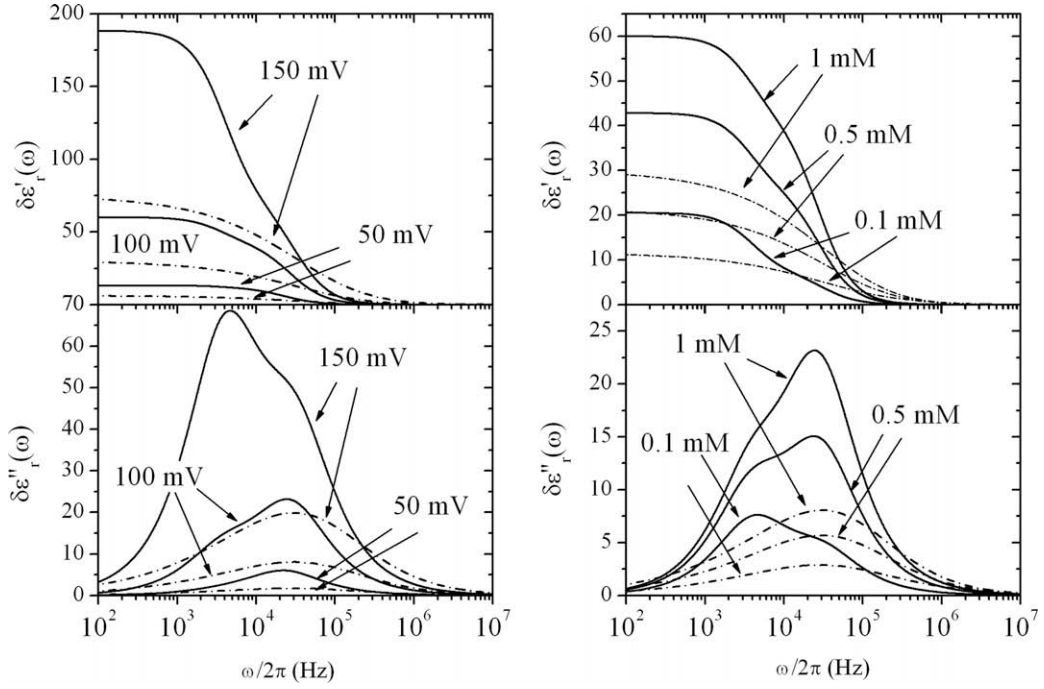

Fig. 3. Real and imaginary components of the electric permittivity increment of goethite suspensions as a function of the frequency of the applied electric field for different values of the zeta potential (left) and the KCl molar concentration (right), according to the predictions of Model I (solid lines) and Model II (dash-dotted lines). Left: 1% volume fraction of solids; b = 100 nm; 1 mM KCl; r = 10. Right: 1% volume fraction of solids; ζ = 100 mV; b = 100 nm; r = 10.

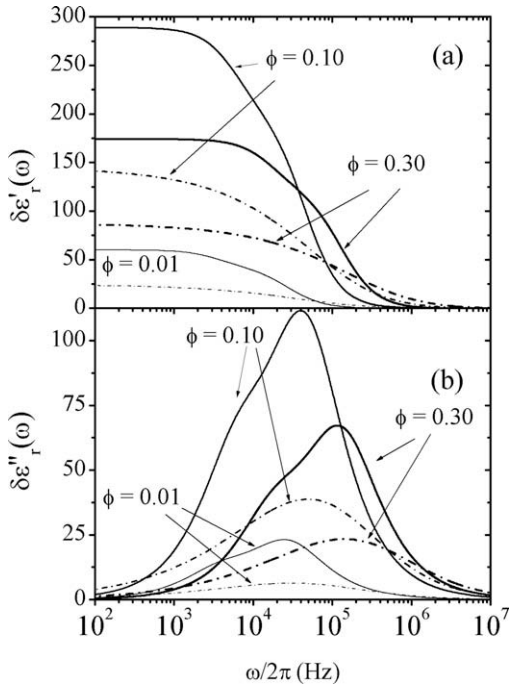

Fig. 4. Real (a) and imaginary (b) parts of the electric permittivity increment of goethite suspensions as a function of the frequency of the applied electric field for different volume fraction of solids. Model I: solid lines; Model II: dash-dotted lines. Other parameters: ζ = 100 mV; b = 100 nm; 1 mM KCl; r = 10.

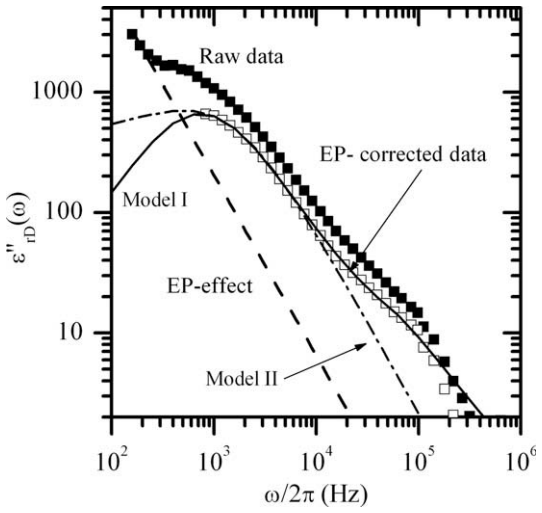

Fig. 5. Logarithmic derivative of the real part of the measured electric permittivity (symbols) and best fits to models (lines) for a suspension containing 4% volume fraction of goethite particles, in a pH 4, 0.5 mM solution of KCl. Full squares: raw data; open squares: data corrected for electrode polarization (EP); solid lines: Model I; dash-dotted lines: Model II. The dashed straight line shows the expected $\omega^{-3/2}$ EP effect.

obtained by the least-squares method, using four adjustable parameters, namely, the semiaxes dimensions (a and b) and two zeta potentials, one corresponding to the parallel orientation $\zeta_{\parallel}$, and one to the perpendicular direction $\zeta_{\perp}$. The sizes characterize the relaxation frequencies, while the necessity of two zeta potentials in the case of spheroids was already pointed out by Jiménez et al. [35], considering that the equipotential surface in spheroidal geometry is not at constant distance to the spheroidal surface, while the ideal stagnant (electrokinetic) plane most likely is. In addition, the use of two zeta potentials can be specially suitable in order to take into account that the goethite particles used appear to be non-uniformly charged [28].

The plots in Fig. 5 show some features which are worth to consider: (i) the uncorrected logarithmic derivative of the permittivity displays huge values in the low-frequency range, which gives us an idea of the importance of electrode polarization; (ii) the correction applied seems to be satisfactory, and, at least above 1 kHz, the

permittivity data appear to be mostly free of the perturbing EP effects; (iii) a large absorption peak is observed in the kHz region in both corrected and uncorrected data, which is well fitted by both models; (iv) a smaller amplitude peak (note the logarithmic scale), at a frequency around 100 kHz, is also noticeable. This smaller peak is properly represented by Model I but not by Model II, which cannot describe a system with two different α-relaxations. We note also that for these systems we detected the characteristic frequency of the Maxwell–Wagner-O'Konski relaxation in the MHz range by means of electro-acoustic techniques [20], so we can affirm that the relaxations observed correspond actually to two alpha relaxations.

4.3. Electric permittivity and ionic strength

The effect of ionic strength on the electric permittivity of goethite rods is shown in Fig. 6: the dielectric increment increases with increasing ionic strength, while no changes in the characteristic frequency are observed. The insets show amplifications of the zones corresponding to the high-frequency peak, where it is seen again that, in accordance with Model I, two relaxation processes appear to be necessary for properly characterizing the dielectric spectrum of our goethite particles.

From the application of the models to this dataset we obtained the parameters in Table 1 (in this and subsequent Tables the error interval is estimated based on the experimental uncertainties – standard deviations of data corresponding to different runs: 10% on average). The first thing that we may note is that Model I predicts two different values for $\zeta_\parallel$ and $\zeta_\perp$, while those obtained by Model II are almost identical. Furthermore, fits to Model II are completely independent from the value of a, and because of that no result is shown for this axis. Concerning the effect of the ionic strength on the obtained zeta potential, almost constant values are returned by Model I while a decreasing trend is given by Model II. This result is expected from the fact that a larger electrolyte concentration produces a greater compression of the EDL around the particles, resulting in a reduction of the zeta potential. Such behavior was also observed from dynamic mobility measurements in our previous work [20], although the reduction in zeta potential was in fact very small in this range of ionic strengths, in agreement with the almost constant value of zeta provided by Model I.

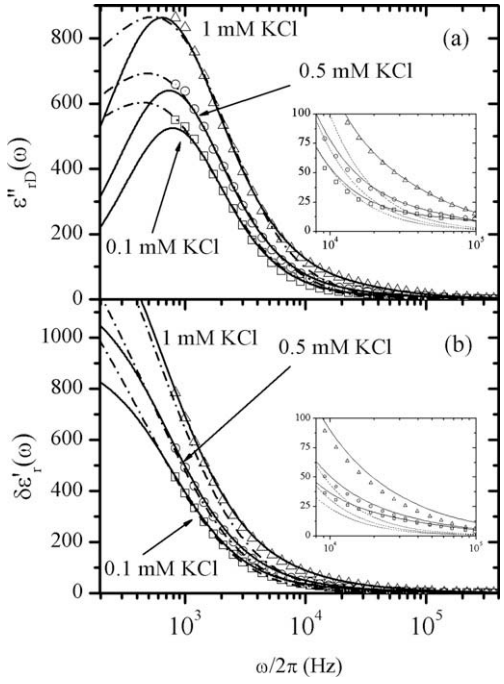

Fig. 6. (a) Experimental data (symbols) for the logarithmic derivative of the real part of the electric permittivity and best fits to models (lines) for a suspension containing 4% volume fraction of goethite particles, in pH 4 solutions with different ionic strengths. Solid lines: Model I; dash-dotted lines: Model II. (b) The same as (a), but for the real part of the electric permittivity.

Table 1
Best-fit values of the zeta potentials ($\zeta_\parallel$ and $\zeta_\perp$), and the two semi-axis (a and b) corresponding to the data in Fig. 6. Volume fraction of solids: 4%; pH 4.

Ionic strength (mM KCl)	$\zeta_\parallel$(mV)		$\zeta_\perp$(mV)	
	Model I	Model II	Model I	Model II
0.1	90 ± 10	200 ± 15	3 ± 2	180 ± 20
0.5	90 ± 10	140 ± 15	3 ± 2	140 ± 20
1	100 ± 15	145 ± 12	3 ± 2	130 ± 15
	a (nm)		b (nm)	
	Model I	Model II	Model I	Model II
0.1	3200 ± 300	–	40 ± 5	1100 ± 200
0.5	3300 ± 300	–	50 ± 6	1000 ± 180
1	3400 ± 350	–	60 ± 7	1000 ± 190

Analyzing the values for the characteristic sizes, the point to consider refers to the unexpectedly large values returned for a by Model I and for b by Model II, which do not correspond with the sizes measured by either light scattering or electron microscopy. It is worth to realize that both values are obtained from the same experimental information: they refer to the characteristic size given by the low-frequency peak, as it is the most important and the only considered by Model II. Such large values can be attributed to the fact that aqueous goethite suspension tend to be flocculated [28], hence the measured size can be related to the presence of aggregates and not just individual particles. Concerning the high-frequency peak, the size calculated by Model I properly agrees with the value of b given by the observation of SEM pictures. The slight increase of b with ionic strength can be attributed to an artifact coming from the limited accuracy of the fits due to the large differences in the amplitudes of both peaks, the high-frequency one being partially hidden by the low-frequency tail.

It seems hence reasonable to attribute the low-frequency peak to both the major axis of individual particles, and to flocs, whereas the high frequency one would correspond to the polarization around single particles oriented perpendicularly to the applied field. Having this in mind, it is tempting to interpret the small value of the high-frequency dielectric increment and its corresponding zeta potential experimentally observed: aggregates comprise most of the particles in suspension, and few particles remain as single entities capable to get individually polarized. This means that Eq. (6), which assumes a random distribution of single spheroidal particles, is not strictly valid. The fact that different zeta potentials are predicted for different regions of the particle surface (and, in particular, that the value corresponding to the lateral face is larger than that on the tips of the rods) confirms the non-uniform surface charge distribution.

4.4. pH effects

Prior to analyze these results, we must point out that a huge quantity of base had to be added to the solution in order to get the values 6 and 8 for the pH, with the subsequent increase in the concentration of ions in solution. Thus, in order to properly control the ionic strength for all the suspensions, we had to increase it up to 5 mM KCl, in an attempt to reduce the contribution of the ions added with the base. As a consequence, electrode polarization was very significant in such conditions: this is the reason why the data in Fig. 7 only display the high-frequency relaxation,

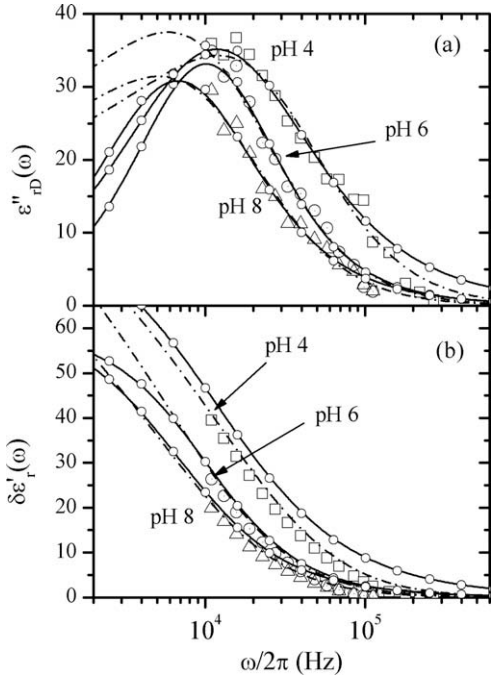

Fig. 7. (a) Experimental data (symbols) of the logarithmic derivative of the real part of the electric permittivity and best fits to models (lines) of suspensions of goethite particles for different pH values. Other parameters: 4% volume content of solids; ionic strength 5 mM KCl. Solid lines: Model I; dashed-dotted lines: Model II. (b) The same as (a), but for the real part of the relative permittivity increment.

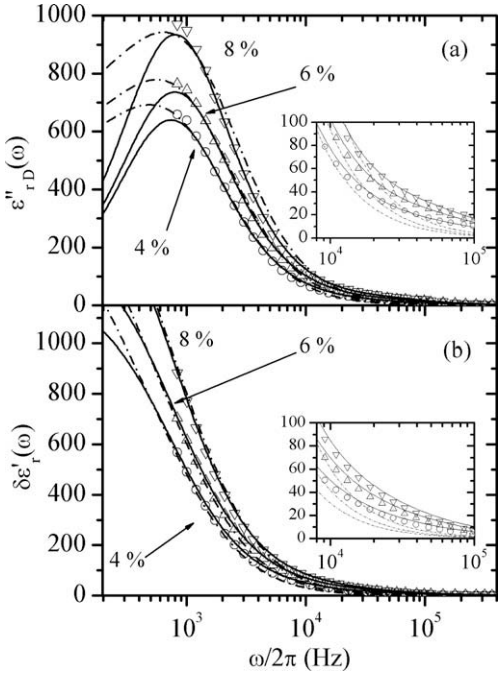

Fig. 8. As in Fig. 7, but for different volume fractions of solids in suspension. Other parameters: pH 4; ionic strength 0.5 mM KCl.

as the low-frequency peak of the spectrum is hidden by the polarization. In addition, the tail of the polarization relaxation is also present in the data and probably leads to an overestimation of the amplitude of the high-frequency one (note the large difference between the values of $\zeta_\perp$ provided by Model I in Table 1 and those given in Table 2). The information in Fig. 7 shows that the peaks appear at lower frequencies than in previous cases, thus returning higher values of the calculated sizes (see Table 2). Note that the maximum of the high frequency peak in Fig. 5 is around 10^5 Hz, while here it appears to have shifted to $\sim 10^4$ Hz. This shift is due to the aggregation induced by the lowered surface potential as we approach the isoelectric point, which has been reported to be around pH 9 by other authors [28,36,37] and found to be above pH 8 by us [20]. As a consequence, a decrease in the zeta potential upon increasing the pH is returned by the fits (Table 2) to both models.

4.5. Volume fraction effects

Fig. 8 shows how the dielectric spectrum is influenced by the volume fraction of solids. In the analyzed range, only an increase of the dielectric increment is observed, without any effect on the characteristic frequency. This is not surprising, as for the studied range of volume fractions the theoretical treatment predicts almost no influence of volume fraction on the relaxation frequency.

Table 2
Best-fit values of the zeta potential $\zeta_\perp$ and the short semi-axis b corresponding to the data in Fig. 7. Volume fraction of solids: 4%; ionic strength: 5 mM KCl.

pH	$\zeta_\perp$ (mV)		b (nm)	
	Model I	Model II	Model I	Model II
4	18 ± 9	60 ± 8	150 ± 20	220 ± 30
6	15 ± 9	55 ± 6	170 ± 20	310 ± 35
8	15 ± 10	50 ± 7	200 ± 30	330 ± 40

In addition, numerical calculations [12] have shown that the permittivity increment changes from an increasing to a decreasing trend with volume fraction when this is above around 15% of solids.

From the fits to Models I and II we obtained the parameters in Table 3. An almost constant value of the zeta potential is obtained in all cases except in $\zeta_\parallel$ from Model I. This indicates that the formulas (10,11) seem to be applicable in this range of volume fractions, despite all the non-idealities characteristic of the goethite particles. The slightly larger sizes obtained with increasing volume fraction, an opposite behavior to the theoretically expected one, reveals an enhancement of the flocculation among particles. This competition between the effect of volume fraction on the available space around particles and their tendency to form larger flocs yields in turn the observed constant value of the relaxation frequency.

5. Conclusions

In this work we have described experimental results on the electric permittivity of suspensions of goethite particles with volume fractions up to 8% in solids. The results have been compared

Table 3
Best-fit values of the zeta potentials ($\zeta_\parallel$ and $\zeta_\perp$), and the two semi-axis (a and b) corresponding to the data in Fig. 8. Ionic strength: 0.5 mM KCl; pH 4.

Volume fraction	$\zeta_\parallel$(mV)		$\zeta_\perp$(mV)	
	Model I	Model II	Model I	Model II
0.04	90 ± 10	140 ± 15	3 ± 2	140 ± 15
0.06	100 ± 15	140 ± 20	4 ± 3	130 ± 13
0.08	110 ± 12	140 ± 15	4 ± 2	140 ± 20
	a (nm)		b (nm)	
	Model I	Model II	Model I	Model II
0.04	3300 ± 400	–	50 ± 8	1000 ± 200
0.06	3300 ± 400	–	50 ± 7	1000 ± 150
0.08	3300 ± 400	–	50 ± 6	1000 ± 200

to the predictions of two existing theoretical models for the electric permittivity of suspensions of spheroidal particles and extend them in order to account for finite volume fractions. The main difference observed between the two models is that one of them predicts two relaxation processes while the other only one. The experiments have shown that two α-relaxations are clearly observed. The high-frequency one is associated to the short axis of the single particles, as fits to Model I returns a value for the characteristic size compatible with the obtained from SEM pictures. The low-frequency one seems to be related to both the larger axis of individual particles, and to the flocs observed in goethite suspensions by other authors.

Fitting the experimental data to the models allows a coherent characterization of the employed particles regarding the effects of ionic strength, pH and volume fraction. It is worth to note that, although the correction used to incorporate finite volume fractions was not a priori applicable to our system, it has been shown to accurately model the observed behavior.

Acknowledgments

Financial support from Junta de Andalucía, Spain (Project PE-2008-FQM-3993), ESF (Cost Action D43) and MICINN (for a FPU grant to R.A. Rica) is gratefully acknowledged.

Appendix A

Here we give a short account of the expressions required for the calculation of $\delta\varepsilon_r'(0)$ as obtained from Model I. We restrict ourselves to the main results. Readers interested in a wider discussion are referred to the original paper [16].

The dielectric increment (per unit volume fraction) of a dilute suspension of prolate spheroids and the characteristic frequency of the α-relaxation are given by ($i \equiv \|, \perp$):

$$\Delta\varepsilon_{r,d}^{i}(0) = \frac{3\varepsilon_{rm}\kappa^2}{16\pi a b^2}(\gamma^{+,i} - \gamma^{-,i})^2 I^i \tag{A.1}$$

$$\omega_{\alpha,d}^{i} = \frac{16\pi a b^2 (C_{\infty}^{i} - C^i(0))}{\kappa^2(\gamma^{+,i} - \gamma^{-,i})^2 I^i}\,\frac{K_m}{\varepsilon_0\varepsilon_{rm}} \tag{A.2}$$

and the limiting values for the dipolar coefficient:

$$\begin{aligned} C^i(0) &= \tfrac{\gamma^{+,i}+\gamma^{-,i}}{2ab^2} \\ C^i(\infty) &= \tfrac{K_p^{+,i}+K_p^{-,i}-K_m}{3\left(K_m+(K_p^{+,i}+K_p^{-,i}-K_m)L^i\right)} \end{aligned} \tag{A.3}$$

Other quantities depending on the orientation of the spheroid ($i = \|, \perp$) are expressed as follows for a prolate one:

$$\begin{aligned} I^{\|} &= \tfrac{3\pi}{5h^6}\left[-a^3b^2\ln^2\tfrac{a+h}{a-h} + 2hb^2(a^2+b^2)\ln\tfrac{a+h}{a-h} + 4ah^2(a^2-2b^2)\right] \\ I^{\perp} &= \tfrac{3\pi}{20h^6}\left[-ab^4\ln^2\tfrac{a+h}{a-h} + 4h(a^4+h^4)\ln\tfrac{a+h}{a-h} - 4ah^2(3a^2-2b^2)\right] \end{aligned} \tag{A.4}$$

$$\gamma^{\pm,i} = \frac{ab^2}{3}\,\frac{K_p^{\pm,i} - K_m/2}{K_m/2 + (K_p^{\pm,i} - K_m/2)L^i} \tag{A.5}$$

$$h = \sqrt{a^2 - b^2} \tag{A.6}$$

$$\begin{aligned} K_p^{\pm,\|} &= \tfrac{3K^{\sigma,\pm}a}{2bh}\left(\tfrac{a^2-2b^2}{h^2} - \arctan\tfrac{h}{b} + \tfrac{b}{h}\right) \\ K_p^{\pm,\perp} &= \tfrac{3K^{\sigma,\pm}a}{2bh}\left(\tfrac{a^2}{2h^2}\operatorname{arccot}\tfrac{b}{h} + \tfrac{b(a^2-2b^2)}{2a^2h}\right) \end{aligned} \tag{A.7}$$

$$\begin{aligned} L^{\|} &= \tfrac{ab^2}{h^3}(\operatorname{arctanh}\tfrac{h}{a} - \tfrac{h}{a}) \\ L^{\perp} &= \tfrac{1-L^{\|}}{2} \end{aligned} \tag{A.8}$$

Here $K_p^{\pm,i}$ are the contribution of cations (+) and anions (−) to the equivalent conductivity of the particles and L^i are the depolarization factors for prolate spheroids.

Appendix B

Based on Model II [17], the electric permittivity is obtained from the dipolar coefficient, which is expressed as:

$$C^i(\omega) = \frac{K_p^* - K_m^* + 3(1-L^i)[K^{\|} + K^U] + 3L^iK^{\perp}}{3K_m^* + 3L^i(K_p^* - K_m^*) + 9L^i(1-L^i)\left[K^{\|}(b/r_0)^3 + K^U(b/r_1)^3 - K^{\perp}\right]} \tag{A.9}$$

For the sake of brevity, only the definitions of the parameters involved are defined below. For a wider discussion on their derivation and physical meaning, see original paper [16].

$$\begin{aligned} K_m^* &= K_m + j\omega\varepsilon_{rm}\varepsilon_0 \\ K_p^* &= j\omega\varepsilon_{rp}\varepsilon_0 \end{aligned} \tag{A.10}$$

$$\begin{aligned} K^{\|} &= -K_m I_{n,eq} - \tfrac{2J_1K_m\left[I_{c,eq}^2 - I_{n,eq}^2\right]}{J_2(r_0/b)^3\exp[\lambda_n(r_0-b)]} \\ K^{\perp} &= \tfrac{2J_1K_mI_{n,eq}}{J_2(r_0/b)^3\exp[\lambda_n(r_0-b)]} \end{aligned} \tag{A.11}$$

$$\begin{aligned} I_{n,eq} &= \tfrac{-1}{b^2}\int_b^{r_0} x\left[\cosh\left(\tfrac{e\Psi_{eq}}{k_BT}\right) - 1\right]dx \\ I_{c,eq} &= \tfrac{1}{b^2}\int_b^{r_0} x\left[\sinh\left(\tfrac{e\Psi_{eq}}{k_BT}\right) - 1\right]dx \end{aligned} \tag{A.12}$$

$$\begin{aligned} r_0 &= b + \kappa^{-1}\left(1 + \tfrac{3}{\kappa b}\exp(-e\zeta/2k_BT)\right) \\ r_1 &= b + \kappa^{-1}\tfrac{2.5}{1+2\exp(-\kappa b)} \end{aligned} \tag{A.13}$$

In these integrals $\Psi_{eq}(r)$ is the equilibrium electric potential at distance r of the center of a spherical particle of radius b, and $x = (r - b)$. Other parameters needed are:

$$\begin{aligned} \lambda_n &= \sqrt{\tfrac{j\omega}{D}} \\ J_1 &= 1 + \lambda_n r_0 \\ J_2 &= 2 + 2\lambda_n b + \lambda_n^2 b^2 \end{aligned} \tag{A.14}$$

Finally, it is important to write correctly the following equation, which appeared with two misprints in the original paper[1]:

$$\begin{aligned} K^U &= -K_m m\tfrac{e\zeta}{k_BT}I_{c,eq}\left[\tfrac{I_{n,eq} - \gamma I_{c,eq} + 1/2}{(I_{n,eq} - \gamma I_{c,eq}) - J_2/(2J_1)(r_0/b)^3\exp(\lambda_n(r_0-b))} - 1\right] \\ (\gamma &= I_{n,eq}/I_{c,eq}) \end{aligned} \tag{A.15}$$

References

[1] S.S. Dukhin, V.N. Shilov, Dielectric Phenomena and the Double Layer in Disperse Systems and Polyelectrolytes, Wiley, New York, 1974.
[2] S.S. Dukhin, V.N. Shilov, Adv. Colloid Interface Sci. 13 (1980) 153.
[3] M. Fixman, J. Chem. Phys. 124 (2006) 214506.
[4] M.C. Fair, J.L. Anderson, Langmuir 8 (1992) 2850.
[5] M. Guerin, J.C. Seaman, Clays Clay Miner. 52 (2004) 145.
[6] R.J. Hunter, J.C. Seaman, in: A. Hubbard (Ed.), Encyclopedia of Colloid and Surface Science, Marcel Dekker, New York, 2002.

[1] The misprints were: the absence of the minus sign at the beginning of the expression, and the +1/2 addend in the numerator in brackets, which in the original paper appears as −1/4. Note that the former error was already noted in our previous work about dynamic mobility [19], but unluckily we did not detect the second one. In spite of this mistake, results presented in that work are accurately correct, as our checks have proved that the second mistake mentioned mainly influences the low-frequency part of the spectrum.

[7] R.B. McKay (Ed.), Technological Applications of Dispersions, Marcel Dekker, New York, 1994.
[8] M.M. Springer, A. Korteweg, J. Lyklema, J. Electroanal. Chem. 153 (1983) 55.
[9] M. Fixman, J. Chem. Phys. 72 (1980) 5177.
[10] C. Grosse, in: A.V. Delgado (Ed.), Interfacial Electrokinetics and Electrophoresis, Marcel Dekker, New York, 2002, pp. 277–327.
[11] E.H.B. DeLacey, L.R. White, J. Chem. Soc. Faraday Trans. II 77 (1981) 2007.
[12] F. Carrique, F.J. Arroyo, M.L. Jiménez, A.V. Delgado, J. Chem. Phys. 118 (2003) 1945.
[13] A.V. Delgado, F.J. Arroyo, F. Carrique, M.L. Jiménez, J. Phys. – Condens. Matter 12 (2000) A233.
[14] F.J. Arroyo, F. Carrique, M.L. Jiménez, A.V. Delgado, J. Colloid Interface Sci. 229 (2000) 118.
[15] C. Chassagne, F. Mietta, J.C. Winterwerp, J. Colloid Interface Sci. 336 (2009) 352.
[16] C. Grosse, S. Pedrosa, V.N. Shilov, J. Colloid Interface Sci. 220 (1999) 31.
[17] C. Chassagne, D.J. Bedeaux, J. Colloid Interface Sci. 326 (2008) 326.
[18] M.L. Jiménez, F.J. Arroyo, A.V. Delgado, F. Mantegazza, T. Bellini, R. Rica, J. Colloid Interface Sci. 309 (2007) 296.
[19] A.V. Delgado, F.J. Arroyo, F. González-Caballero, V.N. Shilov, Y.B. Borkovskaya, Colloids Surf. A 140 (1998) 139.
[20] R.A. Rica, M.L. Jiménez, A.V. Delgado, Langmuir 25 (2009) 10587.
[21] V.N. Shilov, A.V. Delgado, F. González-Caballero, J. Horno, J.J. López-García, C. Grosse, J. Colloid Interface Sci. 232 (2000) 141.
[22] F.J. Arroyo, F. Carrique, S. Ahualli, A.V. Delgado, Phys. Chem. Chem. Phys. 6 (2004) 1446.
[23] S. Ahualli, A.V. Delgado, S.J. Miklavcic, L.R. White, Langmuir 22 (2006) 7041.
[24] A. Keizer, W.P.J. van der Drift, J.Th.G. Overbeek, Biophys. Chem. 3 (1975) 107.
[25] L.D. Landau, E.M. Lifshitz, L.P. Pitaevskii, Electrodynamics of Continuous Media, Pergamon, Oxford, 1984.
[26] C.J.F. Böttcher, P. Bordewijk, Theory of Electric Polarization, vol. 2, Elsevier, Amsterdam, 1978.
[27] M. Medebach, C. Moitzi, N. Freiberger, O.J. Glatter, J. Colloid Interface Sci. 305 (2007) 88.
[28] B.C. Blakey, D.F. James, Colloids Surf. A 231 (2003) 19.
[29] M.C. Tirado, F.J. Arroyo, A.V. Delgado, C. Grosse, J. Colloid Interface Sci. 227 (2000) 227.
[30] L.A. Rosen, D.A. Saville, Langmuir 7 (1991) 36.
[31] Yu Feldman, E. Polygalov, I. Ermolina, Yu. Polevaya, B. Tsentsiper, Meas. Sci. Technol. 12 (2001) 1355.
[32] M.L. Jiménez, F.J. Arroyo, J. van Turnhout, A.V. Delgado, J. Colloid Interface Sci. 249 (2002) 327.
[33] F. Carrique, F.J. Arroyo, A.V. Delgado, J. Colloid Interface Sci. 206 (1998) 569.
[34] T. Bellini, F. Mantegazza, in: A.V. Delgado (Ed.), Interfacial Electrokinetics and Electrophoresis, Marcel Dekker, New Cork, 2002 (Chapter 14).
[35] M.L. Jiménez, F.J. Arroyo, F. Carrique, U. Kaatze, J. Phys. Chem. B 107 (2003) 12192.
[36] J. Antelo, M. Avena, S. Fiol, R. López, F. Arce, J. Colloid Interface Sci. 285 (2005) 476.
[37] S.J. Allison, J. Colloid Interface Sci. 332 (2009) 1.